

different contributions to the *o*-xylene polarization. Some *o*-xylene would be formed as a geminate recombination product from **11** (eq 11), which is generated by rearrangement of benzvalene radical cations such as **6**, **7**, or **8** in the presence of the semiquinone anion (eq 10). This pathway can be expected to result in strong emission for the methyl protons and weaker emission for the aromatic protons. Another fraction of the *o*-xylene would be formed from free 3,4-dimethylbenzvalene radical cations which have been separated by diffusion from their semiquinone counterions (eq 12). This fraction would carry mainly the polarization complementary to that observed **2**, i.e., enhanced absorption both for the aromatic and methyl protons. The sum of these two contributions may well be the weak absorption observed for the aromatic protons and a fortuitous cancellation of the methyl polarization. Additional support for this scheme is found in the reaction of **1** with photoexcited fluoranil. In this system, the methyl groups of *o*-xylene appear in emission, since the balance of these contributions is now perturbed. The xylene polarization is further complicated by the fact that **2** and *o*-xylene, formed by the

mechanism discussed above, may reenter the photochemical reaction cycle and generate different contributions to the *o*-xylene polarization. Experimentally, the methyl groups appear in increasing emission after several seconds of irradiation time.

Conclusion

The radical-cation rearrangement of **1** stands in marked contrast to its thermal rearrangement. These results illustrate several interesting differences between the (CH)₆ energy surface and that of the corresponding radical cations. It is generally recognized that the barriers to radical-cation rearrangements are lower than the corresponding barriers in the parent system. It is also known that the stabilities of isomeric radical cations may be reversed relative to the neutral diamagnetic parents. Our results indicate, furthermore, that the relative barrier heights for the reorganization of a given radical cation to several different isomers may show an ordering different from those on the parent energy surface.

Registry No. **1**, 31707-64-9; **1** radical cation, 96443-79-7; **2**, 55711-03-0; chloranil, 118-75-2; *o*-xylene, 95-47-6; *m*-xylene, 108-38-3.

Synthesis and Structures of (C₅H₅)₂Mo₂Fe_xTe₂(CO)₇ (x = 1, 2). Cluster Assembly Mechanisms and the Role of the Tellurium

Leonard E. Bogan, Jr.,[†] Thomas B. Rauchfuss,^{*†} and Arnold L. Rheingold^{*†}

Contribution from the School of Chemical Sciences, University of Illinois, Urbana, Illinois 61801, and the Department of Chemistry, University of Delaware, Newark, Delaware 19711. Received April 13, 1984

Abstract: The compound Cp₂Mo₂FeTe₂(CO)₇ (Cp = η⁵-C₅H₅), **2**, is formed in high yield from the reaction of Fe₃Te₂(CO)₉ and Cp₂Mo₂(CO)₆ in hexane under CO. The product was characterized by spectroscopic methods and its structure determined by X-ray crystallography. Compound **2** crystallizes in the P $\bar{1}$ space group with *a* = 13.216 (2) Å, *b* = 15.962 (3) Å, *c* = 21.710 (5) Å, α = 100.31 (2)°, β = 104.74 (2)°, γ = 94.20 (1)°. Z = 8, and ρ_{calcd} = 2.547 g cm⁻³. The structure was solved by direct methods. Blocked cascade refinement on 9947 reflections (*F*_o ≥ 3σ*F*_o) produced the final residuals *R*_F = 0.0354 and *R*_W = 0.0394. The four molecules per asymmetric unit are quite similar, each consisting of a CpMo(CO)₂ fragment bridging the Te wing tips of a Cp(CO)₅MoFeTe₂ butterfly. The 3.13-Å Te...Te distance is well within bonding distance and is proposed to be chemically significant. This interaction is discussed in the context of other nonmetal-containing cluster compounds. On the basis of these data, it is proposed that such intracenter nonmetal-nonmetal interactions can have a significant influence on the structures and reactivity of compounds in this class of clusters. The mechanism of formation of **2** is discussed in light of the recently reported compound Co₂Fe₂S₂(CO)₁₁. Thermolysis of **2** affords metallatetrahedrane Cp₂Mo₂FeTe(CO)₇, Cp₂Mo₂Fe₂Te₃(CO)₆, and Cp₂Mo₂Fe₂Te₂(CO)₇, **3**. Compound **3** crystallizes in the orthorhombic space group Pn2₁a with *a* = 13.617 Å, *b* = 12.939 Å, *c* = 12.199 Å, Z = 4°, (10)°, and ρ_{calcd} = 2.73 g cm⁻³. The structure was solved by direct methods. Blocked cascade refinement on 1837 reflections (*F*_o > 3σ*F*_o) produced *R*_F = 0.0256 and *R*_W = 0.0249. The molecule of approximately C_{2v} symmetry consists of a tetrahedral Mo₂Fe₂ core with each Mo₂Fe face capped by a μ₃-Te atom. The Fe-Fe distance of 2.433 Å is one of the shortest known single Fe-Fe bonds. The mechanism of formation of **3** from **2** was shown to involve no scrambling of Mo moieties (Cp-labeling experiments) and proceeds optimally (60%) in the presence of 10 equiv of Fe(CO)₅. Compound **2** also reacts with CpCo(CO)₂ to give two isomers of Cp₃Mo₂CoFeTe₂(CO)₅. These results imply that the recently reported isomers of Cp₂Mo₂Fe₂S₂(CO)₈ are formed via a five-vertex Mo₂FeS₂ intermediate.

Tellurium-bridged transition metal carbonyl clusters are notably stable in less highly condensed geometries than clusters derived from lighter nonmetals. However, the way that main group atoms influence the connectivity within transition metal-main group carbonyl clusters (TMMGCCs) is poorly understood. Schmid¹ has noted that for clusters of the core stoichiometry (MG)Co₃, only those nonmetals whose covalent radius is less than 1.30 Å exist in the fully condensed, noncarbonyl form. Co₂FeTe(CO)₉ extends this series as this tetrahedral cluster features a large (*r*_{cov}

= 1.37 Å) Te atom capping a closed Co₂Fe triangle with M-M distances of 2.60 Å.² The compound Fe₃(μ₃-SnFe(C₅H₅)(CO)₂)₂(CO)₉ is a more spectacular example of a potentially strained cluster, as the large (*r*_{cov} = 1.41 Å) Sn atoms cap a Fe₃ triangle with an average Fe-Fe bond length of 2.79 Å in this *closo*-trigonal bipyramid.³ The effect of MG size on M-M bond

(1) Schmid, G. *Angew. Chem., Int. Ed. Engl.* **1978**, *17*, 392.

(2) Strouse, C. E.; Dahl, L. F. *J. Am. Chem. Soc.* **1971**, *93*, 6032.

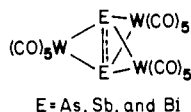
(3) McNeese, T. J.; Wreford, S. S.; Tipton, D. L.; Bau, R. *J. Chem. Soc., Chem. Commun.* **1977**, 390.

[†] University of Illinois. [‡] University of Delaware.

lengths is also apparent in the series of *nido*-Fe₃E₂(CO)₉ clusters (E = NR, S, Se, and Te).⁴

Lewis acidity is a characteristic of many TMMGCCs although it is rare for the binary metal carbonyls. This ability to form adducts, is, however, peculiar to only certain TM-MG combinations (e.g., Fe₃Te₂(CO)₉ but not Fe₃S₂(CO)₉) for reasons which are not yet known. In other publications,⁵ we have emphasized the possible influence of the size of the main group component upon the facility of adduct formation for TM(MG)₂CCs. The present study directs attention to the likelihood of attractive MG...MG interactions as a driving force in some adduct forming reactions.

Intracluster MG...MG bonding interactions must be considered for those clusters which contain more than one MG vertex. Dahl and co-workers have explicitly noted the possibility of such interactions in Co₄(PPh)₂(CO)₁₀,⁶ where the P...P distance of 2.544 Å is 1.256 Å shorter than the sum of the van der Waals radii and only 0.3 Å longer than the accepted P-P single bond distance.⁷ This issue has come into sharper focus as a consequence of the recent work on the five-vertex clusters E₂(W(CO)₅)₃ (E = As, Sb, and Bi), which in fact possess no TM...TM bonds but, based on structural data, have MG...MG bond orders >1.⁸ MG...MG



bonding interactions are also of substantial importance in understanding the structures and reactivity of bimetallic complexes such as Fe₂E₂(CO)₆ (E = S, PR, Se, and Te),^{5a,9} Cp₂Mo₂S₄,¹⁰ and Cp₂V₂S₄ (Cp = η⁵-C₅H₅).¹¹ The role of main group elements in directing both chemical and structural patterns in TMMGCC chemistry is an emerging issue in inorganic chemistry.¹²

The recent discovery of the first examples of isomeric TMMGCCs which differ in their connectivity raises questions about cluster assembly mechanisms.¹³ The ability of TMTECCs

to add, eliminate, and substitute TM vertexes^{5,14} renders this class of compounds especially suitable for such mechanistic studies. The present work provides a rational but nonobvious assembly mechanism which highlights the lability of TM vertexes in TMMGCCs.

Experimental Section

The high-pressure reaction was carried out in a 40-mL screw-cap high-pressure reaction vessel made of 316 SS, and the pyrolysis reaction. Solvents were purged with CO or N₂. Workups were carried out in air. Fe₃Te₂(CO)₉ was prepared as previously reported,^{5a,15} Cp₂Mo₂(CO)₆ was purchased from Pressure Chemical Co. and recrystallized from CH₂Cl₂/hexane before use. ¹H NMR spectra were recorded at 90 MHz on a Varian EM-390 spectrometer or at 200.057 MHz on a Varian XL-200 spectrometer. ¹²⁵Te NMR spectra were recorded at 31.547 MHz on a Varian XL-100 spectrometer. ¹³C NMR spectra were recorded at 90.550 MHz on a Nicolet NT-360 spectrometer. Infrared spectra were recorded on a Nicolet 5-MX spectrometer as solutions in cyclohexane, except where noted. Mass spectra were recorded by Mr. Carter Cook at the University of Illinois on a Finnigan-MAT CH-5 (EI), 731 (FD), or ZAB (FAB) mass spectrometer. Elemental analyses were performed as a departmental service.

Preparation of Cp₂Mo₂FeTe₂(CO)₇ (2). Fe₃Te₂(CO)₉ (0.445 g, 0.659 mmol) and Cp₂Mo₂(CO)₆ (0.323 g, 0.659 mmol) were stirred in 35 mL of hexane for 16 h at 170 °C under 1550 psi CO. The reaction mixture was cooled, vented, and filtered. The precipitate was washed with hexane and then recrystallized from CH₂Cl₂/hexane to yield 0.418 g (0.503 mmol, 76%) of Cp₂Mo₂FeTe₂(CO)₇. Anal. Calcd C, 24.62; H, 1.22; Te, 30.78; Fe, 6.74. Found C, 24.30; H, 0.99; Te, 29.8; Fe, 6.98. FABMS, *m/e* 830 (M⁺), 802, 774, 746, 718, 690, 662, 634; IR 2044 (vs), 1986 (s), 1922 (m), 1848 (m) cm⁻¹; ¹H NMR (CDCl₃) δ 5.88 (s), 5.41 (s); ¹²⁵Te NMR (CDCl₃) δ -1092 (s); ¹³C NMR (CDCl₃, 25 °C) δ 250 (s), 223 (s), 93 (s), 89 (s); (toluene-*d*₆, -61 °C) δ 251 (s), 223 (s), 218 (s), 204 (s), 93 (s), 89 (s). The preparation of Cp₂Mo₂FeTe₂(CO)₇, 2', from Fe₃Te₂(CO)₉ and Cp₂'Mo₂(CO)₆ was completely analogous.

Isolation of Cp₂Mo₂FeTe(CO)₇. Chromatography (silica, CH₂Cl₂-hexane 3:7) of the filtrate from the preparation of Cp₂Mo₂FeTe₂(CO)₇ gave first Cp₂Mo₂FeTe₂(CO)₆ followed closely by a faint red band, Cp₂Mo₂FeTe₂(CO)₇, and finally Cp₂Mo₂FeTe(CO)₇, in very low yield (0.0089 g, 0.0127 mmol, 1%). Anal. Calcd for Cp₂Mo₂FeTe(CO)₇: C, 29.10; H, 1.44. Found: C, 29.06; H, 1.30. EIMS, *m/e* 702 (M⁺), 674, 646, 618, 590, 562, 534, 506; IR 2025 (s), 1975 (m), 1956 (m), 1946 (m), 1937 (m) cm⁻¹; ¹H NMR (CDCl₃) δ 5.22 (s). Anal. Calcd for Cp₂Mo₂FeTe₂(CO)₆: C, 19.52; H, 1.02. Found: C, 19.66; H, 0.98. FDMS, *m/e* 986 (M⁺); IR 2020 (m), 2008 (w), 1991 (s), 1946 (vs), 1686 (m) cm⁻¹; ¹H NMR (CDCl₃) δ 4.60 (s).

Thermolysis of 2. Compound 2 (0.3548 g, 0.428 mmol) was refluxed under either N₂ or CO (both gave the same result) in 120 mL of toluene for 2 h. The resulting mixture was chromatographed (silica, CH₂Cl₂-hexane 1:1), yielding golden Cp₂Mo₂FeTe₂(CO)₆ (0.0152 g, 0.0154 mmol, 3.6%), followed closely by a faint red band, green 2 (0.0194 g, 0.0234 mmol, 5.5%), purple Cp₂Mo₂FeTe(CO)₇ (0.0079 g, 0.11 mmol, 2.6%), and finally purple Cp₂Mo₂FeTe₂(CO)₇, 3 (0.0226 g, 0.0255 mmol, 6.0% after recrystallization from CH₂Cl₂/MeOH). Anal. Calcd for Cp₂Mo₂FeTe₂(CO)₆: C, 19.52; H, 1.02. Found: C, 19.61; H, 0.88. FDMS *m/e* 985 (M⁺); IR 2009 (w), 1991 (s), 1948 (m), 1941 (m) cm⁻¹; ¹H NMR δ 4.60 (s). Anal. Calcd for 3: C, 23.07; H, 1.14. Found: C, 23.09; H, 1.14. FDMS, *m/e* 886 (M⁺); IR (CH₂Cl₂) 2014 (vs), 1987 (s), 1952 (br, s) 1825 (br, w), 1723 (br, m) cm⁻¹; ¹H NMR δ 5.35, 5.08 (s).

Reaction of 2 with Fe(CO)₅. Compounds 2' (Cp₂'Mo₂FeTe₂(CO)₇, Cp' = CH₃C₅H₄) (0.407 g, 0.475 mmol) and Fe(CO)₅ (0.630 mL, 4.74 mmol) were refluxed in 70 mL of toluene for 1.5 h. Workup as above gave Fe₃Te₂(CO)₉ (0.0073 g, 0.011 mmol, 2.3%), Cp₂'Mo₂FeTe₂(CO)₆ (0.0088 g, 0.009 mmol, 1.8%), 2'' (0.030 g, 0.035 mmol, 7.4%), Cp₂'Mo₂FeTe(CO)₇ (0.0064 g, 0.009 mmol, 1.8%), and 3'' (0.2616 g, 0.287 mmol, 60%). When the experiment was repeated with only 1 equiv of Fe(CO)₅, it yielded Cp₂'Mo₂FeTe₂(CO)₆ (6%), 2'' (15%), Cp₂'Mo₂FeTe(CO)₇ (2.1%), and 3'' (29%).

Reaction of 2 with CpCo(CO)₂. Compounds 2 (0.4357 g, 0.5255 mmol) and CpCo(CO)₂ (0.150 mL) were refluxed in 130 mL of toluene for 2.5 h. Workup as above gave Cp₂Mo₂CoFeTe₂(CO)₅ (0.090 g, 0.10 mmol, 19% after recrystallization from CH₂Cl₂/MeOH). Anal. Calcd: C, 26.77; H, 1.69. Found: C, 25.89; H, 1.69. FDMS, *m/e* 897, 755

(14) Bogan, L. E., Jr.; Lesch, D. A.; Rauchfuss, T. B. *J. Organomet. Chem.* **1983**, *250*, 429.

(15) Bogan, L. E., Jr.; Day, V. W.; Lesch, D. A.; Rauchfuss, T. B., unpublished results.

(4) (a) Schumann, H.; Magerstädt, M.; Pickardt, J. *J. Organomet. Chem.* **1982**, *240*, 407. (b) Huntsman, J. R. Ph.D. Thesis, University of Wisconsin, Madison, 1973. (c) Dahl, L. F.; Sutton, P. W. *Inorg. Chem.* **1963**, *2*, 1067. (d) Jacob, J.; Weiss, E. *J. Organomet. Chem.* **1977**, *131*, 263. (e) Doedens, R. *J. Inorg. Chem.* **1969**, *8*, 570.

(5) (a) Lesch, D. A.; Rauchfuss, T. B. *Inorg. Chem.* **1981**, *20*, 3583. (b) Lesch, D. A.; Rauchfuss, T. B. *Organometallics* **1982**, *1*, 499. (c) Day, V. W.; Lesch, D. A.; Rauchfuss, T. B. *J. Am. Chem. Soc.* **1982**, *104*, 1290. (d) Lesch, D. A.; Rauchfuss, T. B. *J. Organomet. Chem.* **1980**, *199*, C6. (e) Lesch, D. A.; Rauchfuss, T. B. *Inorg. Chem.* **1983**, *22*, 1854.

(6) Ryan, R. C.; Pittman, Jr., C. U.; O'Connor, J. P.; Dahl, L. F. *J. Organomet. Chem.* **1980**, *193*, 247.

(7) Additional examples of significantly short NM...NM interactions are found in [Co₄(η⁵-C₅H₅)₄(μ₃-P)₄], P...P 2.568 Å (av);⁸ [Fe₄(CO)₁₀(μ₄-P-*p*-tolyl)P(OMe)₂], P...P 2.598 (3) Å;⁶ [Fe₄(CO)₁₁(μ₄-P-*p*-tolyl)₂P(OMe)₃], P...P 2.598 (3) Å;⁶ [Rh₄(μ₄-PC₆H₅)₂(COD)₂], P...P 2.679 (4) Å;⁶ [(CO)₃Fe]₂(C₆H₅)₄, P₁...P₂ 2.715 (3) Å;⁶ [(CO)₃Fe]₂(PC₆H₅)₄, P₁...P₄ 2.689 (1) Å;⁶ [(C-CO)₃Fe]₂(AsCH₃)₄, As₁...As₄ 2.895 (4) Å;⁶ [CpMo(CO)₂]₂(AsCH₃)₅, As₁...As₅ 2.835 (2) Å.⁶ (a) Simon, G. L.; Dahl, L. F. *J. Am. Chem. Soc.* **1973**, *95*, 2175. (b) Vahrenkamp, H.; Wolters, D. *Organometallics* **1982**, *1*, 873. (c) Burkhardt, E. W.; Mercer, W. C.; Geoffroy, G. L.; Rheingold, A. L.; Fultz, W. C. *J. Chem. Soc., Chem. Commun.* **1983**, 1251. (d) Rheingold, A. L.; Fountain, M. A. *Organometallics* submitted. (e) Gatehouse, B. M. *J. Chem. Soc., Chem. Commun.* **1969**, 948. (f) Rheingold, A. L.; Churchill, M. R. *J. Organomet. Chem.* **1983**, *243*, 165.

(8) (a) Sigwarth, B.; Zsolnai, L.; Berke, H.; Huttner, G. *J. Organomet. Chem.* **1982**, *226*, C5. (b) Huttner, G.; Weber, U.; Sigwarth, B.; Scheidsteger, O. *Angew. Chem., Int. Ed. Engl.* **1982**, *21*, 215. (c) Huttner, G.; Weber, U.; Zsolnai, L. *Z. Naturforsch.* **1982**, *37b*, 707.

(9) (a) Campana, C. F.; Lo, F. Y. K.; Dahl, L. F. *Inorg. Chem.* **1979**, *18*, 3060. (b) Vahrenkamp, H.; Wolters, D. *Angew. Chem., Int. Ed. Engl.* **1983**, *22*, 154.

(10) Brunner, H.; Meier, W.; Wachter, J.; Guggolz, E.; Zahn, T.; Ziegler, M. L. *Organometallics* **1982**, *1*, 1107.

(11) Bolinger, C. M.; Rauchfuss, T. B. *J. Am. Chem. Soc.* **1983**, *105*, 6321.

(12) The concept of attractive MG...MG bonding is supported by molecular orbital calculations. Cowley, A. J.; Dewar, M. J. S.; Lattman, M.; Mills, J. L.; McKee, M. *J. Am. Chem. Soc.* **1978**, *100*, 3349. Teo, B. K.; Hall, M. B.; Fenske, R. F.; Dahl, L. F. *Inorg. Chem.* **1975**, *14*, 3103.

(13) (a) Braunstein, P.; Jud, J. M.; Tiripicchio, A.; Tiripicchio-Camellini, M.; Sappa, E. *Angew. Chem., Int. Ed. Engl.* **1982**, *21*, 307. (b) Williams, P. D.; Curtis, M. D.; Duffy, D. N.; Butler, W. D. *Organometallics* **1983**, *2*, 165.

Table I. Crystal and Refinement Data

| | compound 2 | compound 3 |
|---|--|-------------------------------|
| formula | $C_{17}H_{10}FeMo_2O_7Te_2$ | $C_{17}H_{10}Fe_2Mo_2O_7Te_2$ |
| fw | 829.03 | 885.0 |
| crystal system | triclinic | orthorhombic |
| space group | $P\bar{1}$ | $Pn2_1a$ |
| <i>a</i> , Å | 13.216 (2) | 13.617 (3) |
| <i>b</i> , Å | 15.962 (3) | 12.939 (3) |
| <i>c</i> , Å | 21.710 (5) | 12.199 (3) |
| α , deg | 100.31 (2) | 90 |
| β , deg | 104.74 (2) | 90 |
| γ , deg | 94.20 (1) | 90 |
| <i>V</i> , Å ³ | 4323.5 (16) | 2149.4 |
| <i>Z</i> | 8 | 4 |
| ρ_{obsd} , ρ_{calcd} , g cm ⁻³ | 2.6, 2.547 | 2.5, 2.73 |
| temp, °C | 23 | 23 |
| crystal dimension, mm | 0.26 × 0.29 × 0.30 | 0.28 × 0.31 × 0.32 |
| radiation | graphite-mono-chromated Mo K α ($\lambda = 0.71073$ Å) | same |
| diffractometer | Nicolet R3 | same |
| abs coeff, cm ⁻¹ | 45.53 | 52.3 |
| scan speed, deg/min | var. 3.0–12.0 | same |
| 2 θ scan range, deg | 4° < 2 θ < 45° | 4° < 2 θ < 50° |
| scan technique | $\theta - 2\theta$ | ω |
| data collected | $\pm h, \pm k, +l$ | <i>hkl</i> |
| scan width, deg | 0.8 + $\Delta(\alpha_1 - \alpha_2)$ | same |
| unique data | 11,401 reflns (11,979 collected) | 1989 (2179) |
| unique data with $F_{obsd}^2 > 3\delta F_{obsd}^2$ | 9,947 | 1837 |
| std reflns | 3/197 (<1.0% decay) | 3/97 (<2%) |
| R_F | 0.0354 | 0.0256 |
| R_{wF} | 0.0394 | 0.0249 |
| GOF | 1.254 | 1.361 |

(M^+ , $M^+ - 5CO$); ¹H NMR δ 5.38 (s), 5.30 (s), 5.06 (s), 4.84 (s) (14:7:86:43); IR (CH₂Cl₂) 1983 (s), 1912 (m), 1813 (m) cm⁻¹.

Test for Exchange of CpMo Fragments. The Cp₂' (Cp' = CH₃C₅H₄) analogues of the three products of the thermolysis of **2** were prepared from Cp₂'Mo₂FeTe₂(CO)₇. FABMS of an equimolar mixture of Cp₂ and Cp₂' derivatives of the Mo₂FeTe₃ cluster showed none of the mixed (CpCp') isomer. Similarly, neither EIMS of **3** and **3'** nor FDMS of the Cp₂ and Cp' derivatives of the Mo₂FeTe cluster showed any mixed isomers. An equimolar mixture of **2** and **2''** was thermolyzed, and the products were separated and analyzed by mass spectrometry. *In no case was any mixed isomer detected.*

Reaction of Cp₂Mo₂(CO)₄ with Fe₂S₂(CO)₆. A solution of Cp₂Mo₂(CO)₄ (0.0665 g, 0.176 mmol) in 2.5 mL of toluene was added dropwise to a solution of Fe₂S₂(CO)₆, **10** (0.6059 g, 1.762 mmol, 10 equiv), in 1.0 mL of toluene at 0 °C. After stirring at 0 °C for 20 min, the Fe_xS₂(CO)_y clusters were separated from the reaction mixture by column chromatography. The resulting mixture was analyzed by IR spectroscopy and found to contain 0.019 mmol (11%) of Fe₃S₂(CO)₉. The yield of Fe₃S₂(CO)₉ was markedly sensitive to the concentrations of the reactants and to the rate of addition. Two other trials afforded 31% and 4.3% yields of Fe₃S₂(CO)₉.

Reaction of Cp₂Mo₂(CO)₆ with Fe₃S₂(CO)₉. Fe₃S₂(CO)₉ (0.222 g, 0.459 mmol), Cp₂Mo₂(CO)₆ (0.225 g, 0.459 mmol), and hexane (90 mL) were heated at 180 °C under 1750 psi of CO for 15 h. After venting and cooling the autoclave, the reaction mixture was filtered and the residue washed with hexane. Extraction of the residue with CH₂Cl₂ and crystallization from CH₂Cl₂/hexane afforded *cis*-Cp₂Mo₂Fe₂S₂(CO)₈ (0.165 g, 0.229 mmol, 50%) identified by mass spectroscopy and comparison of its IR spectrum with that of an authentic sample. FDMS: 720 (M^+). IR(CH₂Cl₂): 2052 (m), 2025 (s), 1981 (sh), 1971 (m), 1807 (w). Similar results were obtained when Fe₂(S₂)(CO)₆ was used in place of Fe₃S₂(CO)₉. None of the trans isomer was present in the reaction mixture. In a separate experiment it was shown that the trans isomer is quantitatively converted to the *cis* isomer upon heating for 4 h at 150 °C under 1700 psi of CO.

X-ray Structure Determination of 2. (a) **Collection and Processing of Intensity Data.** A black specimen was trimmed to a nearly cubic form (0.28-mm edge) and affixed to a fine glass fiber. The unit-cell parameters reported in Table I were obtained from the angular settings of 25 Friedel-related reflections (25° ≤ 2 θ ≤ 32°). The intensity data were corrected for Lp effects and for absorption by an empirical, ψ -scan technique (max/min transmission 0.117/0.073). A learned profile analysis of all reflections was used to improve the precision in the mea-

surement of weak reflections. Averaging of redundant data after correction for absorption showed a disagreement of less than 1.0%. The choice of the centrosymmetric triclinic space group $P\bar{1}$ was initially based upon the E statistics and later confirmed by the successful and chemically reasonable solution and refinement of the structure. All programs used in data collection, solution, and refinement are contained in the P3 and SHELXTL (version 3.0) packages provided by the Nicolet Corp.

(b) **Solution and Refinement of the Structure.** The structure was eventually solved by the direct methods routine SOLV after overcoming what appeared to be origin definition problems. A solution with the third highest combined figures of merit (from a total of 128) provided the positions of all 20 Te, Mo, and Fe atoms in the four independent molecules. The remaining C and O atoms were located in a subsequent difference Fourier synthesis. In the final cycles of blocked-cascade refinement, 846 parameters were refined by using those 9947 reflections with $F_0 \geq 3\sigma F_0$. All non-hydrogen atoms except the Cp ring carbon atoms were refined with ellipsoidal thermal parameters, and hydrogen atoms were included in idealized and updated locations ($d(C-H) = 0.96$ Å) but not refined. The top ten peaks on the final difference map ($u.1-0.8$ e Å³) were all associated with various of the eight Cp rings and undoubtedly indicate the presence of minor (<20%), disordered orientations of the rings. Since no unusual aspects of the major ring-carbon atom locations, thermal parameters, or of the ring shapes were found, no attempt was made to model the disorder. No chemically significant differences exist in the four independent molecules. Selected bond distances and angles are provided in Table II. A complete listing of bond distances and angles, fractional atomic coordinates, anisotropic temperature factors, and observed vs. calculated structure factors are available as supplementary material.

X-ray Structure Determination of 3. (a) **Collection and Processing of Intensity Data.** Black crystals of Cp₂Mo₂Fe₂Te₂(CO)₇ were affixed to glass fibers and the unit cell parameters and crystal system determined from the angular settings of 25 reflections (25° ≤ 2 θ ≤ 30°). These data along with experimental conditions and refinement data are provided in Table I. The intensity data were corrected for Lp effects and for the absorption by an empirical, ψ -scan technique (XMT) (max/min transmission, 0.165/0.140). This and all other programs used in collection, solution, and refinement of the data are contained in the P3 and SHELXTL (version 3.0) packages provided by the Nicolet Corp. Systematic absences in the reflection data indicated either the centrosymmetric space group $Pnma$ or the noncentrosymmetric alternative $Pn2_1a$ (nonstandard setting for $Pna2_1$). In $Pnma$, the crystallographically required mirror plane molecular symmetry would contain the two Fe and two Te atoms, which is clearly not compatible with the actual structure. Curiously, the cluster does contain a nearly perfect mirror plane perpendicular to the crystallographically required axis defined by the Mo atoms, the centroids of the Cp rings, and the μ -CO ligand, C(1)-O(1), and C(2)-O(2). Statistics based upon E 's also strongly supported the noncentrosymmetric alternative, which was ultimately verified by the well-behaved and chemically reasonable refinement of the structure.

(b) **Solution and Refinement of the Structure.** The structure was solved by the direct methods routine SOLV after numerous trial and error adjustments to parity group representations in the starting set had been made. Eventually a solution containing the positions of Te, Mo, and Fe atoms was used to obtain the remaining nonhydrogen atoms by difference Fourier syntheses. The model used in the final cycles of blocked-cascade, least-squares refinement included a correction in secondary extinction and employed anisotropic temperature factors for all non-hydrogen atoms except for the Cp ring carbon atoms, hydrogen atoms included as fixed, idealized contributions ($d(C-H) \approx 0.96$ Å) and converged at $R_F = 0.0256$ and $R_{wF} = 0.0249$, for those 1901 reflections with $F_{obsd} \geq 3F_{obsd}$, giving a data/parameter ratio of 8.6/1. In the last cycle, the mean-shift/esd maximum was 0.123 and the three highest peaks on the final difference map, 0.61–0.81 e Å⁻³, were located around the perimeter of the Cp rings, suggesting the presence of minor rotational disorder in the rings. Selected bond distances and angles are provided in Table III. A complete listing of bond distances and angles, fractional atomic coordinates, anisotropic temperature factors, and observed vs. calculated structure factors are available as supplementary material.

Results

Synthesis of Mo₂FeTe_x Clusters ($x = 1$ and 2). The reaction of equimolar quantities of Fe₃Te₂(CO)₉, **1**, and Cp₂Mo₂(CO)₆ at 170 °C under 1550 psi CO afforded a new compound with the formula Cp₂Mo₂FeTe₂(CO)₇, **2**. Compound **2** proved to be air-stable in the solid state and was readily obtained as dark green crystals. ¹H and ¹²⁵Te NMR spectroscopies indicated non-equivalent Cp groups and equivalent Te atoms. The ¹²⁵Te resonance was in the chemical shift range of *arachno*-M₃Te₂ clusters.^{5e}

Table II. Selected Bond Distances, Angles, and Dihedral Angles for $\text{Cp}_2\text{Mo}_2\text{Fe}(\mu_3\text{-Te})_2(\text{CO})_7$

| bond | mol 1 | mol 2 | mol 3 | mol 4 | |
|-------------------------------------|-------------------|------------|------------|------------|-----------|
| Bond Distances, Å | | | | | |
| Mo(1)–Te(1) | 2.781 (1) | 2.772 (1) | 2.775 (1) | 2.787 (1) | |
| Mo(1)–Te(2) | 2.780 (1) | 2.780 (1) | 2.793 (1) | 2.779 (1) | |
| Mo(2)–Te(1) | 2.822 (1) | 2.812 (1) | 2.808 (1) | 2.832 (1) | |
| Mo(2)–Te(2) | 2.816 (1) | 2.811 (1) | 2.807 (1) | 2.810 (1) | |
| Fe–Te(1) | 2.584 (1) | 2.581 (1) | 2.575 (1) | 2.588 (1) | |
| Fe–Te(2) | 2.582 (1) | 2.584 (1) | 2.579 (1) | 2.572 (1) | |
| Te(1)⋯Te(2) | 3.146 (1) | 3.150 (1) | 3.134 (1) | 3.136 (1) | |
| Mo(1)–Fe | 2.850 (1) | 2.843 (1) | 2.846 (1) | 2.828 (1) | |
| Mo(1)⋯Mo(2) | 4.271 (1) | 4.255 (1) | 4.272 (1) | 4.289 (1) | |
| Mo(2)⋯Fe | 4.170 (1) | 4.161 (1) | 4.158 (1) | 4.184 (1) | |
| CNT(1)–Mo(1) | 1.984 (9) | 1.996 (9) | 1.980 (9) | 1.978 (9) | |
| CNT(2)–Mo(2) | 2.009 (10) | 2.004 (11) | 2.009 (9) | 2.009 (10) | |
| Mo(1)–C(14) | 1.983 (9) | 2.014 (9) | 1.964 (11) | 1.986 (9) | |
| Mo(1)–C(15) | 2.009 (10) | 2.006 (11) | 1.990 (8) | 2.004 (11) | |
| Mo(2)–C(16) | 1.949 (9) | 1.944 (8) | 1.932 (9) | 1.934 (8) | |
| Mo(2)–C(17) | 1.952 (8) | 1.958 (9) | 1.936 (9) | 1.941 (10) | |
| Fe–C(11) | 1.763 (8) | 1.766 (10) | 1.761 (10) | 1.755 (8) | |
| Fe–C(12) | 1.811 (10) | 1.787 (10) | 1.818 (11) | 1.769 (9) | |
| Fe–C(13) | 1.794 (10) | 1.772 (8) | 1.786 (10) | 1.785 (12) | |
| Bond Angles, deg | | | | | |
| Te(1)–Mo(1)–Te(2) | 68.9 (0) | 69.1 (0) | 68.5 (0) | 68.6 (0) | |
| Te(1)–Mo(2)–Te(2) | 67.8 (0) | 68.1 (0) | 67.8 (0) | 67.5 (0) | |
| Te(1)–Fe–Te(2) | 75.0 (0) | 75.2 (0) | 74.9 (0) | 74.8 (0) | |
| Mo(1)–Te(1)–Mo(2) | 99.3 (0) | 99.3 (0) | 99.9 (0) | 99.5 (0) | |
| Mo(1)–Te(2)–Mo(2) | 99.5 (0) | 99.1 (0) | 99.4 (0) | 100.2 (0) | |
| Te(1)–Mo(1)–Fe | 54.6 (0) | 54.7 (0) | 54.5 (0) | 54.9 (0) | |
| Te(2)–Mo(1)–Fe | 54.6 (0) | 54.7 (0) | 54.4 (0) | 54.6 (0) | |
| Mo(1)–Te(1)–Fe | 64.1 (0) | 64.0 (0) | 64.1 (0) | 63.3 (0) | |
| Mo(1)–Te(2)–Fe | 64.1 (0) | 63.9 (0) | 63.8 (0) | 63.7 (0) | |
| Mo(2)–Te(1)–Fe | 100.9 (0) | 100.8 (0) | 101.2 (0) | 101.0 (0) | |
| Mo(2)–Te(2)–Fe | 101.1 (0) | 100.8 (0) | 101.1 (0) | 101.9 (0) | |
| CNT(1)–Mo(1)–Te(1) | 115.8 (4) | 115.0 (3) | 118.7 (3) | 115.4 (4) | |
| CNT(1)–Mo(1)–Te(2) | 115.8 (3) | 116.4 (3) | 114.5 (3) | 116.3 (3) | |
| CNT(1)–Mo(1)–Fe | 167.2 (4) | 167.1 (4) | 167.7 (3) | 167.5 (4) | |
| CNT(1)–Mo(1)–C(14) | 112.6 (4) | 112.7 (3) | 111.7 (4) | 110.9 (3) | |
| CNT(1)–Mo(1)–C(15) | 111.7 (4) | 112.5 (3) | 111.8 (3) | 112.1 (4) | |
| CNT(2)–Mo(2)–Te(1) | 118.3 (4) | 116.8 (4) | 117.4 (4) | 118.7 (4) | |
| CNT(2)–Mo(2)–Te(2) | 116.7 (4) | 119.3 (3) | 119.6 (3) | 118.2 (4) | |
| CNT(2)–Mo(2)–C(16) | 121.9 (7) | 118.7 (6) | 122.0 (7) | 121.3 (6) | |
| CNT(2)–Mo(2)–C(17) | 120.4 (6) | 120.5 (7) | 120.3 (7) | 120.4 (6) | |
| C(14)–Mo(1)–C(15) | 85.3 (4) | 84.0 (4) | 83.2 (4) | 84.1 (4) | |
| C(16)–Mo(2)–C(17) | 76.6 (4) | 79.4 (4) | 78.5 (4) | 77.8 (4) | |
| Mo(1)–Fe–Te(1) | 61.3 (0) | 61.2 (0) | 61.3 (0) | 61.8 (0) | |
| Mo(1)–Fe–Te(2) | 61.3 (0) | 61.4 (0) | 61.7 (0) | 61.7 (0) | |
| Mo(1)–Fe–C(11) | 149.7 (3) | 148.3 (3) | 149.8 (3) | 149.4 (3) | |
| Mo(1)–Fe–C(12) | 103.5 (3) | 105.3 (3) | 104.7 (3) | 104.0 (2) | |
| Mo(1)–Fe–C(13) | 104.2 (3) | 106.6 (3) | 102.1 (3) | 104.9 (3) | |
| C(11)–Fe–C(12) | 97.1 (4) | 96.4 (5) | 96.3 (5) | 95.9 (4) | |
| C(11)–Fe–C(13) | 95.7 (4) | 94.2 (4) | 96.6 (4) | 95.8 (4) | |
| C(12)–Fe–C(13) | 95.1 (4) | 94.4 (4) | 97.0 (5) | 95.7 (5) | |
| C(11)–Fe–Te(1) | 95.5 (3) | 94.0 (3) | 93.2 (4) | 95.0 (3) | |
| C(11)–Fe–Te(2) | 95.5 (3) | 94.8 (3) | 97.7 (3) | 94.5 (3) | |
| C(12)–Fe–Te(1) | 164.2 (3) | 166.5 (3) | 162.3 (3) | 164.5 (3) | |
| C(12)–Fe–Te(2) | 94.3 (3) | 96.5 (3) | 89.1 (3) | 93.3 (3) | |
| C(13)–Fe–Te(1) | 93.1 (3) | 92.3 (4) | 96.6 (4) | 94.1 (4) | |
| C(13)–Fe–Te(2) | 164.4 (3) | 165.5 (3) | 163.8 (3) | 165.5 (3) | |
| Mo(1)–C(14)–O(14) | 172.4 (7) | 173.7 (8) | 172.4 (10) | 173.2 (6) | |
| Mo(1)–C(15)–O(15) | 173.4 (7) | 173.4 (9) | 172.7 (8) | 172.8 (8) | |
| Mo(2)–C(16)–O(16) | 174.8 (9) | 178.2 (8) | 179.2 (8) | 178.2 (8) | |
| Mo(2)–C(17)–O(17) | 177.4 (8) | 178.0 (8) | 176.4 (9) | 176.6 (9) | |
| Fe–C(11)–O(11) | 178.4 (8) | 177.3 (10) | 175.6 (9) | 178.0 (9) | |
| Fe–C(12)–O(12) | 177.2 (9) | 175.9 (7) | 176.4 (10) | 178.4 (7) | |
| Fe–C(13)–O(13) | 177.9 (9) | 179.5 (10) | 177.4 (9) | 176.4 (9) | |
| plane 1 | plane 2 | mol 1 | mol 2 | mol 3 | mol 4 |
| Dihedral Angles between Planes, deg | | | | | |
| Te(1)–Mo(1)–Te(2) | Te(1)–Mo(2)–Te(2) | 134.5 (5) | 134.5 (4) | 134.6 (4) | 134.8 (4) |
| Te(1)–Mo(1)–Te(2) | Te(1)–Fe–Te(2) | 81.9 (4) | 81.8 (4) | 81.6 (5) | 81.6 (4) |
| Te(1)–Mo(2)–Te(2) | Te(1)–Fe–Te(2) | 143.7 (5) | 143.7 (5) | 143.9 (4) | 143.6 (4) |

Solution IR spectra revealed one ν_{CO} at 1848 cm^{-1} and an envelope of ν_{CO} absorptions centered at 1984 cm^{-1} . Solid-state IR spectra were similar. A low-temperature ^{13}C NMR spectrum revealed a four-line pattern in the carbonyl region. These data indicate that the solid-state structure for **2** (vide infra) is maintained in

solution.

Compound **2** does not react with either excess PMe_2Ph or with Me_3NO . It reacts with $\text{Co}_2(\text{CO})_8$ only under forcing conditions and then with low conversion, affording a low yield of $\text{Co}_2\text{FeTe}(\text{CO})_9^2$ and a trace of $\text{CpMoCoFeTe}(\text{CO})_8$.¹⁶ Treatment with

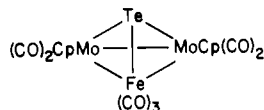
Table III. Selected Bond Distances (Å) and Angles (deg) for $Cp_2Mo_2Fe_2(\mu_3\text{-Te})_2(CO)_7$

| | | | |
|-------------|------------|-------------------|-----------|
| Mo-Co | 2.888 (1) | Mo(1)-Te(1)-Mo(2) | 65.1 |
| Mo(1)-Fe(1) | 2.861 (2) | Mo(1)-Te(1)-Fe(1) | 67.3 |
| Mo(1)-Fe(2) | 2.863 (2) | Mo(2)-Te(1)-Fe(1) | 67.6 |
| Mo(1)-Fe(1) | 2.872 (2) | Mo(1)-Te(2)-Mo(2) | 65.3 |
| Mo(1)-Fe(2) | 2.889 (2) | Mo(1)-Te(2)-Fe(2) | 67.4 |
| Mo(1)-Te(1) | 2.684 (1) | Mo(2)-Te(2)-Fe(2) | 68.2 |
| Mo(1)-Te(2) | 2.683 (1) | Te(1)-Mo(1)-Te(2) | 114.5 |
| Mo(1)-Te(1) | 2.681 (1) | Te(1)-Mo(1)-Mo(2) | 57.4 |
| Mo(1)-Te(2) | 2.673 (1) | Te(1)-Mo(1)-Fe(1) | 52.8 |
| Fe(1)-Te(1) | 2.472 (2) | Te(1)-Mo(1)-Fe(2) | 96.6 |
| Fe(1)-Te(2) | 2.468 (2) | Te(2)-Mo(1)-Mo(2) | 57.2 |
| Fe-Te | 2.433 (2) | Te(2)-Mo(1)-Fe(1) | 96.1 |
| Te...Te | 4.513 | Te(2)-Mo(1)-Fe(2) | 52.7 |
| Fe(1)-C(2) | 1.947 (1)2 | Te(1)-Mo(2)-Te(2) | 114.9 |
| Fe(2)-C(2) | 1.929 (12) | Te(1)-Mo(2)-Mo(1) | 57.5 |
| C(2)-O(2) | 1.191 (16) | Te(1)-Mo(2)-Fe(1) | 52.7 |
| C(4)-O(4) | 1.129 (15) | Te(1)-Mo(2)-Fe(2) | 96.0 |
| Mo(1)-C(1) | 1.982 (11) | Te(2)-Mo(2)-Mo(1) | 57.5 |
| Fe(1)-C(1) | 2.465 (10) | Te(2)-Mo(2)-Fe(1) | 96.0 (1) |
| Fe(1)-C(1) | 2.467 (10) | Te(2)-Mo(2)-Fe(2) | 52.5 |
| C(1)-O(1) | 1.167 (13) | Te(1)-Fe(1)-Mo(1) | 59.9 |
| | | Te(1)-Fe(1)-Mo(2) | 59.7 |
| | | Te(1)-Fe(1)-Fe(2) | 115.2 (1) |
| | | Mo(1)-Fe(1)-Mo(2) | 60.5 |
| | | Mo(1)-Fe(1)-Fe(2) | 64.9 |
| | | Mo(2)-Fe(1)-Fe(2) | 65.4 |
| | | Te(2)-Fe(2)-Mo(1) | 59.9 |
| | | Te(2)-Fe(2)-Mo(2) | 59.2 |
| | | Te(2)-Fe(2)-Fe(1) | 114.6 (1) |
| | | Mo(1)-Fe(2)-Mo(2) | 60.3 |
| | | Mo(1)-Fe(2)-Fe(1) | 64.8 |
| | | Mo(2)-Fe(2)-Fe(1) | 64.7 (1) |
| | | Fe(1)-C(2)-Fe(2) | 77.8 (4) |
| | | Mo(1)-C(1)-Fe(1) | 79.3 (4) |
| | | Mo(1)-C(1)-Fe(2) | 79.3 (4) |
| | | Fe(1)-C(1)-Fe(2) | 59.1 (2) |
| | | Mo(1)-C(1)-O(1) | 156.3 (9) |

Br_2/CO converts **2** into $CpMo(CO)_3Br$ and $CpMoFeTe_2Br(CO)_5$.¹⁷

A compound identified as $Cp_2Mo_2FeTe(CO)_7$ was isolated as a minor product in the preparation of **2**. Its ¹H NMR spectrum indicates equivalent Cp ligands and its infrared spectrum indicates that all the carbonyl ligands are terminal. These observations combined with the well-known stability of $Co_2FeTe(CO)_9$ and the fact that both $Co(CO)_3$ and $CpMo(CO)_2$ are 15e fragments leads us to propose a tetrahedral structure for the Mo_2FeTe core of this cluster.

Three compounds were obtained in low yields upon thermolysis of **2**: a second isomer of $Cp_2Mo_2Fe_2Te_3(CO)_6$, the aforementioned $Cp_2Mo_2FeTe(CO)_7$, and $Cp_2Mo_2Fe_2Te_2(CO)_7$, **3**. It is interesting



to note that the latter two species differ from **2** by the removal or the addition of one atom. There was no change in either the products or the yields when the reaction was carried out under CO instead of N_2 . A labeling experiment was conducted to determine whether CpMo fragments were exchanged during the thermolysis of **2**. The bis-Cp' (Cp' = $CH_3C_5H_4$) derivatives of the thermolysis products were prepared, and mass spectra were recorded for equimolar mixtures of these bis-Cp' compounds and their bis-Cp analogues. In no case was any mixed isomer (CpCp') detected. An equimolar mixture of **2** and $Cp'_2Mo_2FeTe_2(CO)_7$ was then thermolyzed, and the mass spectra of the individual

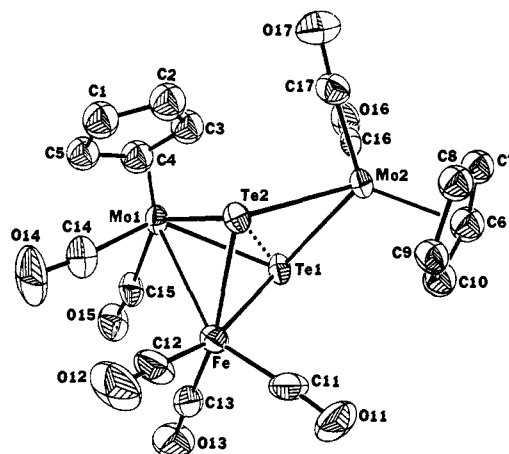


Figure 1. ORTEP plot of the non-hydrogen atoms of a $(C_5H_5)_2Mo_2Fe_2Te_2(CO)_7$ molecule with thermal ellipsoids drawn at the 50% probability level.

products were obtained. Again, no mixed CpCp' isomer was detected.

We expect the structure of the isomer of $Cp_2Mo_2Fe_2Te_3(CO)_6$ obtained by thermolysis of **2** to be analogous to $Cp_2Mo_2Co_2S_3(CO)_4$,¹⁸ although we have not been able to confirm this crystallographically. We determined that the structure of **3** is closely related to one isomer of $Cp_2Mo_2Fe_2S_2(CO)_8$ (vide infra).

The yield of the conversion of **2** to **3** was increased by a factor of 10 to 60% by the addition of 10 equiv of $Fe(CO)_5$ to the reaction mixture. Addition of 1 equiv gave only a 30% yield. Using $CpCo(CO)_2$ instead of $Fe(CO)_5$, a compound identified as $Cp_3Mo_2CoFeTe_2(CO)_5$ was formed from **2**. The ¹H NMR spectrum of this $Mo_2FeCoTe_2$ cluster showed two pairs of Cp resonances, each pair integrating in a ratio of 2:1 and the sums of these pairs integrating in a ratio of 86:14. Because CpCo is isoelectronic and isolobal with $Fe(CO)_3$, we propose that these isomeric Mo_2CoFe clusters are structurally akin to the isomers of $Cp_2Mo_2Fe_2S_2(CO)_8$ formed from the reaction of $Fe_2(S_2)(CO)_6$ and $Cp_2Mo_2(CO)_4$.

We investigated the possibility that free $Fe(CO)_x$ fragments are formed in the reaction of $Fe_2(S_2)(CO)_6$ with $Cp_2Mo_2(CO)_4$. Taking advantage of the fact that $Fe_2(S_2)(CO)_6$ reacts rapidly with $Fe(CO)_x$ ($x < 5$) to give the very stable $Fe_3S_2(CO)_9$, a toluene solution of $Cp_2Mo_2(CO)_4$ was added slowly to a toluene solution of 100 equiv of sublimed $Fe_2(S_2)(CO)_6$. Chromatographic workup of three such reactions revealed formation of significant quantities of $Fe_3S_2(CO)_9$. The yields were variable and dependent on the concentrations of the reactants and the rate of addition.

The reaction of $Fe_3S_2(CO)_9$ and $Cp_2Mo_2(CO)_6$ under conditions identical with those used to prepare **2** gave a good yield of the cis, "Braunstein isomer" of $Cp_2Mo_2Fe_2S_2(CO)_8$.^{13a} Under the conditions of this experiment, the trans, "Curtis isomer" is converted into the cis form.

Structure of $Cp_2Mo_2FeTe_2(CO)_7$ (2**).** A crystal of **2** was grown from CH_2Cl_2 /hexane. Single crystal X-ray diffraction revealed the presence of four independent molecules per asymmetric unit. Each molecule differs only slightly from the others. A representative molecule is depicted in Figure 1 and structural parameters are presented in Table II.

The basic cluster geometry resembles that found for $Fe_3Te_2(CO)_9PPh_3$.^{5b,c} The Mo_2FeTe_2 core adopts the structure predicted for a five-vertex, *arachno* cluster. The carbonyl ligands on the Mo atom bonded to Fe are very slightly semibridging. The low-energy ν_{CO} absorption for **2** is found at 1848 cm^{-1} , 21 cm^{-1} lower than the lowest observed in $Cp_2Mo_2(CO)_4$ ¹⁹ and 44 cm^{-1} lower than the lowest ν_{CO} observed in $Cp_3Mo_3S(CO)_6^+$,²⁰ which has been

(16) Anal. Calcd for $CpMoCoFeTe(CO)_8$: C, 24.88; H, 0.80. Found C, 25.17; H, 0.94. EIMS, m/e 629 (M^+), 601, 573, 545, 517, 489, 461, 433, 405; IR 2068 (m), 2026 (s), 2009 (m), 1992 (m) cm^{-1} ; ¹H NMR ($CDCl_3$) δ 5.41.

(17) Bogan, L. E., Jr.; Rauchfuss, T. B.; Rheingold, A. L., unpublished results.

(18) Curtis, M. D.; Williams, P. D. *Inorg. Chem.* **1983**, *22*, 2661.

(19) Klinger, R. J.; Butler, W.; Curtis, M. D. *J. Am. Chem. Soc.* **1975**, *97*, 3535.

(20) Curtis, M. D.; Butler, W. M. *J. Chem. Soc., Chem. Comm.* **1980**, 998.

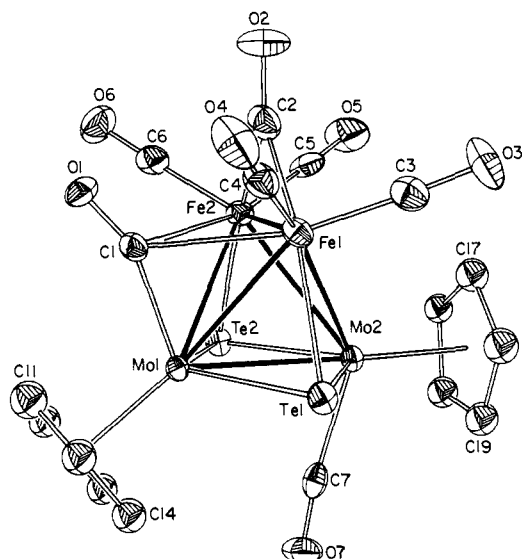


Figure 2. ORTEP plot of the non-hydrogen atoms of a $(C_5H_5)_2Mo_2Fe_2Te_2(CO)_7$ molecule with thermal ellipsoids drawn at the 50% probability level.

classified as "barely semibridding". The average Mo(1)-C-O angle of 172.9° is larger than the 168° in $Cp_3Mo_3S(CO)_6^+$ but smaller than the 175.9° in $Cp_2Mo_2(CO)_4$.

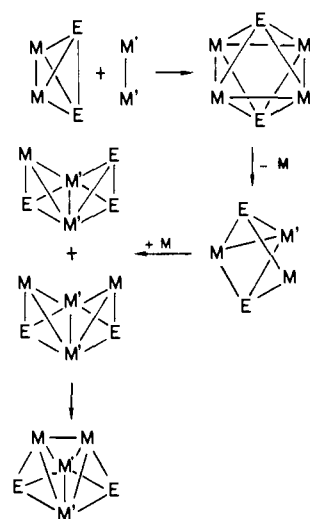
The Fe-Te, Mo-Te, and Fe-Mo bond lengths are unexceptional. The average Fe-Te distance is 2.581 \AA , 0.049 \AA longer than the 2.532 \AA seen in the *nido*- $Fe_2Te_2(CO)_9^{4a}$ but 0.021 \AA shorter than the 2.602 \AA in the *arachno*- $Fe_3Te_2(CO)_9PPh_3$.^{5c} The average Mo-Te distances are 2.781 \AA for Mo(1) and 2.815 \AA for Mo(2), both within the range of 2.698 - 2.816 \AA observed in β - $MoTe_2$.²¹ The average Mo-Fe bond length in the four independent molecules is 2.842 \AA , 0.11 \AA shorter than the Mo-Fe bonds in $[(MeCp)MoS_2Fe(CO)_3]_2^{22}$ but slightly longer than the corresponding bonds in $CpMoCoFeS(CO)_7(PMePrPh)$,²³ $CpMoCo_2FeSAs(CO)_8$,²⁴ or either isomer of $Cp_2Mo_2Fe_2S_2(CO)_8$.¹³ The average nonbonded Mo...Mo and Mo...Fe distances are 4.272 and 4.168 \AA , respectively, too long for significant interaction.

The average Te...Te distance of 3.142 \AA is short. The Te...Te distance in **1** is 3.36 \AA and that for $Fe_3Te_2(CO)_7(PPh_3)_2^{15,25}$ is 3.31 \AA . The PPh_3 adduct of **1** features a short (3.13 \AA) Te...Te distance. A similar trend is seen in the Co_4Te_2 clusters: the d_{TeTe} of 3.30 \AA in $Co_4Te_2(CO)_{10}^{26}$ contracts by 0.26 \AA upon formation of its CO adduct, $Co_4Te_2(CO)_{11}$.²⁷

Structure of $Cp_2Mo_2Fe_2Te_2(CO)_7$ (3**).** A crystal of **3** was grown from $CH_2Cl_2/MeOH$. The molecular structure is depicted in Figure 2, and structural parameters are contained in Table III. The basic cluster geometry consists of a Mo_2Fe_2 tetrahedron with each Mo_2Fe_2 face capped by a μ_3 -Te atom. The structure resembles that of Braunstein's isomer of $Cp_2Mo_2Fe_2S_2(CO)_8^{13a}$ with the loss of one CO ligand compensated for by formation of an Fe-Fe bond which in turn is bridged by CO. One, but not both, of the Mo atoms possesses a semitriply bridging CO ligand like those seen on both Mo atoms in $Cp_2Mo_2Fe_2S_2(CO)_8$. On the other Mo atom, the Cp and CO ligands have essentially exchanged coordination sites and the CO ligand points well away from the cluster. This structure is retained in solution as indicated by the occurrence of two Cp resonances in the 1H NMR spectrum.

The average Mo-Mo, Mo-Fe, Mo-Te, and Fe-Te bond lengths compare well with known standards. The average Fe-Te bond

Scheme I



length of 2.470 \AA is shorter than the 2.532 , 2.542 , and 2.581 \AA seen in **1**,^{4a} $CpMoFeTe_2Br(CO)_5$,¹⁷ and **2**.

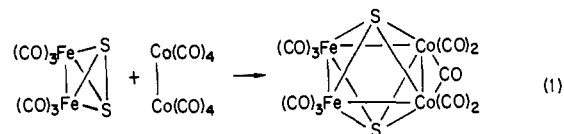
The Fe-Fe bond length of 2.433 \AA is short. This distance is 0.31 \AA shorter than in **1**, and of the $Fe_3E_2(CO)_9$ series, only the compound with $E = NMe$ has Fe-Fe bonds of similar length (2.46 \AA).^{4c} This bond is even shorter than the CO-bridged bond in $Fe_4(PPh)_2(CO)_{11}$ (2.440 \AA),²⁸ to which some multiple-bond character has been ascribed on the basis of the EAN formalism and its ability to form adducts with Lewis bases. It is only 0.107 \AA longer than the formal double bond in $Cp_2Fe_2(NO)_2$.²⁹

The average Fe-C(2) bond of 1.938 \AA is 0.078 \AA shorter than the bridging Fe-C bonds in $Fe_2(CO)_9^{30}$ but close to the 1.93 and 1.96 \AA on the short sides of the Fe-C bridges in $Fe_3(CO)_{12}$.³¹ The C(2)-O(2) bond is a fairly long 1.191 \AA (c.f. 1.176 \AA in $Fe_2(CO)_9$), giving rise to the ν_{CO} at 1723 cm^{-1} in CH_2Cl_2 solution. The remaining carbonyl ligands are unexceptional. The average Fe-CO bond length is 1.760 \AA , slightly shorter than the 1.781 \AA in **2**. The semibridding Mo-CO bond of 1.982 \AA compares well with the 2.025 \AA in $Cp_2Mo_2Fe_2S_2(CO)_8$,^{13a} and the terminal Mo-CO bond of 2.005 \AA is only slightly longer than the 1.969 \AA in **2**.

Discussion

The compounds $Cp_2Mo_2Fe_xTe_2(CO)_7$ ($x = 1$ and 2) are of particular interest with regard to their mechanism of formation and bonding.

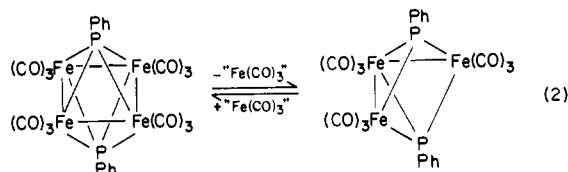
Cluster Assembly. We have previously shown that at elevated temperatures and CO pressures, compound **1** is an efficient source of the highly reactive $Fe_2(Te_2)(CO)_6$ species.¹⁵ The latter compound smoothly adds to low valent metals, affording derivatives featuring the Fe_2Te_2M core ($M = Fe, Co, Rh, Pt,$ and Pd).^{5,15} The formation of $Fe_2(Te_2)(CO)_6$ from the reaction of **1** with $Cp_2Mo_2(CO)_6$ under CO is evidenced by the recovery of both $Fe(CO)_5$ and $Fe_4Te_4(CO)_{12}$ from the reaction mixture.^{5a} In analogy with the recently reported reactions of $Fe_2(S_2)(CO)_6$ with $Cp_2Mo_2(CO)_4$ and $Co_2(CO)_8$ ³² (eq 1), we anticipated that the



(21) Brown, B. E. *Acta Crystallogr.* **1966**, *20*, 268.
 (22) Cowans, B.; Noordik, J.; Rakowski DuBois, M. *Organometallics* **1983**, *2*, 931.
 (23) Richter, F.; Vahrenkamp, H. *Chem. Ber.* **1982**, *115*, 3243.
 (24) Richter, F.; Vahrenkamp, H. *Organometallics* **1982**, *1*, 756.
 (25) Lesch, D. A. Ph.D. Thesis, University of Illinois, Urbana-Champaign, 1982.
 (26) deGil, E. R. Ph.D. Thesis, University of Wisconsin, Madison, 1968.
 (27) Strouse, C. E. Ph.D. Thesis, University of Wisconsin, Madison, 1969.

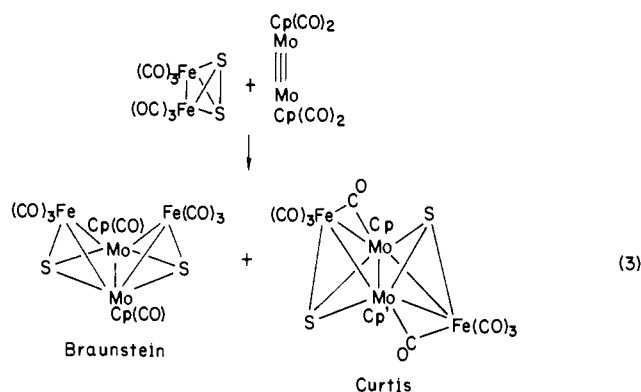
(28) Vahrenkamp, H.; Wolters, D. J. *Organomet. Chem.* **1982**, *224*, C17.
 Vahrenkamp, H.; Wucherer, E. J.; Wolters, D. *Chem. Ber.* **1983**, *116*, 1219.
 (29) Calderón, J. L.; Fontana, S.; Frauendorfer, E.; Day, V. W.; Iske, S. D. A. *J. Organomet. Chem.* **1974**, *64*, C16. Nitrogen bridged iron dimers generally feature short ($<2.43 \text{ \AA}$) Fe-Fe contacts, see: Dahl, L. F.; Costello, W. R.; King, R. B. *J. Am. Chem. Soc.* **1968**, *90*, 5422.
 (30) Cotton, F. A.; Troup, J. M. *J. Chem. Soc. Dalton Trans.* **1974**, 800.
 (31) Cotton, F. A.; Troup, J. M. *J. Am. Chem. Soc.* **1974**, *96*, 4155.

reaction of **1** with $Cp_2Mo_2(CO)_6$ would lead to either octahedral or bitetrahedral $Mo_2Fe_2Te_2$ clusters. We can rationalize the formation of **2** by invoking the loss of an even-electron $Fe(CO)_n$ fragment from an $Mo_2Fe_2Te_2$ intermediate, and in support of this



view we note that $Fe_4(PPh)_2(CO)_{12}$ reversibly dissociates an $Fe(CO)_3$ vertex to give $Fe_3(PPh)_2(CO)_9$ (e.g., eq 2).²⁸ Our proposed assembly mechanism is outlined in Scheme I.

Other aspects of the assembly of **2** and **3** merit comment, the first being their relationship to the isomeric bitetrahedral $Mo_2Fe_2S_2$ clusters recently obtained from $Cp_2Mo_2(CO)_4$ and $Fe_2(S_2)(CO)_6$ (eq 3). The stability of **2** contrasts with the apparent instability



of the corresponding Mo_2FeS_2 cluster. *Arachno* clusters analogous to $Cp_2Mo_2FeS_2(CO)_7$ are unknown and may be unstable with respect to decarbonylation. Recall that $Fe_3S_2(CO)_9$, unlike $Fe_3Te_2(CO)_9$, does not add CO .^{5a} We propose that decarbonylation of $Cp_2Mo_2FeE_2(CO)_7$ triggers the formation of the $Cp_2Mo_2FeE_2(CO)_x$ clusters. In support of this mechanism we observe that the rate of thermal decomposition of **2** is qualitatively the same as the rate of its reaction with $Fe(CO)_5$ to give **3**.

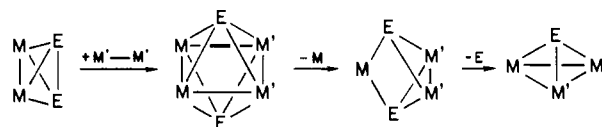
Our experiments suggest that the mechanism of assembly of the Braunstein–Curtis isomers occurs via a Mo_2FeS_2 intermediate. The following results have a bearing on this issue:

- A Cp-labeling study indicates that the conversion of **2** to **3** proceeds *without* splitting of the Mo_2 subunit.
- The yield of the conversion of **2** to **3** increases tenfold (to 60%) upon the addition of 10 equiv of $Fe(CO)_5$.
- The addition of $CpCo(CO)_2$ in place of $Fe(CO)_5$ gives ca. 20% yield of Mo_2FeCo species.
- $Cp_3Mo_2CoFeTe_2(CO)_5$, like the isoelectronic $Mo_2Fe_2S_2$ clusters, was obtained as a mixture of two isomers.
- The reaction of $Cp_2Mo_2(CO)_4$ with excess $Fe_2(S_2)(CO)_6$ affords significant quantities of $Fe_3S_2(CO)_9$, thereby implicating the formation of $Fe(CO)_x$ ($x < 5$) intermediates.
- The trans form of $Cp_2Mo_2Fe_2S_2(CO)_8$ can be thermally isomerized into the cis form.

The formation of $Mo_2Fe_2Te_2$ and isomeric $Mo_2FeCoTe_2$ clusters from the reactions of **2** with $Fe(CO)_5$ and $CpCo(CO)_2$ provides mechanistic clues to the formation of the $Cp_2Mo_2Fe_2S_2(CO)_8$ isomers. The most striking aspect of the mechanistic results described in this paper is the requirement for the dissociation–reassociation of a metal carbonyl fragment. The applicability of the fragmentation mechanism to the Braunstein–Curtis system was demonstrated by trapping the dissociated $Fe(CO)_x$ as $Fe_3S_2(CO)_9$, using a large excess of $Fe_2(S_2)(CO)_6$. This vertex dissociation occurs even at 0 °C and shows that transition metals are not always firmly “glued” together by main group centers.

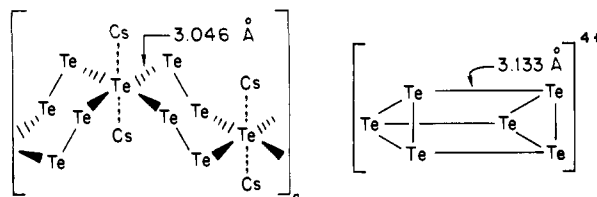
A longstanding mechanistic enigma in this area of chemistry concerns the pathway by which $Co_2FeS(CO)_9$ forms from $Fe_2(S_2)(CO)_6$ and $Co_2(CO)_8$.³³ Our finding that sources of Fe_2-

Scheme II



$Te_2(CO)_6$ react with $[CpMo(CO)_3]_2$ to give **2**, which decomposes without dissociation of the Cp_2Mo_2 unit, to give, *inter alia*, $Cp_2Mo_2FeTe(CO)_7$ suggests the sequence of events depicted in Scheme II.

Intracluster Bonding between Main Group Centers. We have already noted that the average $Te\cdots Te$ distance in **2** of 3.142 Å is short. The $Te\cdots Te$ distance of 2.712 Å in Ph_2Te_2 ³⁴ may be considered a typical single bond length. The nearest-neighbor distances in Te metal are 2.835 Å,³⁵ but interchain interactions at a distance of 3.495 Å are considered to be structurally significant as well.³⁶ The $Te-Te$ bonds about the four-coordinate



Te atoms in Cs_2Te_5 are 3.046 Å,³⁷ while those between the triangular faces in $[Te_6]^{4+}$ average 3.133 Å.³⁶ Valence bond analysis of $[Te_6]^{4+}$ suggests that these intertriangle bonds have a bond order of 2/3.

When $Fe_3Te_2(CO)_9$ forms an adduct with PPh_3 , its $Te\cdots Te$ distance contracts from 3.36 to 3.14 Å. Similarly, when $Co_4Te_2(CO)_{10}$ forms an adduct with CO , its $Te\cdots Te$ distance contracts from 3.30 to 3.06 Å.²⁷ As indicated in the preceding discussions, $Te\cdots Te$ distances of 3.14 and 3.06 Å are well within the known range of strong $Te-Te$ bonding interactions. Compound **2**, with $d(TeTe) = 3.14$ Å, may be thought of as a CO adduct of $Cp_2Mo_2FeTe_2(CO)_6$, an unknown molecule which would presumably have a square pyramidal (nido) Mo_2FeTe_2 core geometry. It may be significant that these clusters all feature short $Te\cdots Te$ interactions subsequent to adduct formation. On the other hand, clusters tethered by smaller and less polarizable atoms, such as $Fe_3S_2(CO)_9$,^{4b} $Fe_3(PPh)_2(CO)_9$,^{4b} and $Co_4S_2(CO)_{10}$,³⁸ show no Lewis acidity. We have previously suggested that the strain inherent in acute $Fe-Te-Fe$ angles destabilizes the $Fe\cdots Fe$ bonding in $Fe_3Te_2(CO)_9$, thereby promoting the formation of adducts.^{5a,b} In view of the present results, attractive $Te\cdots Te$ interactions may contribute to the stabilization of $Fe_3Te_2(CO)_9$, **2**, and $Co_4Te_2(CO)_{10}$.²⁷ Short $MG\cdots MG$ contacts are not sufficient to induce adduct formation in all $(TM)_3(MG)_2$ clusters since $Fe_3(PPh)_2(CO)_9$, with a $P\cdots P$ separation of 2.60 Å^{4b} (0.68 times twice the van der Waals radius), does not form adducts with phosphines. However, $Co_4(PPh)_2(CO)_{10}$ ($d(P\cdots P) = 2.544$ Å) has been claimed to catalyze the hydroformylation of olefins,³⁹ and $Fe_4(PPh)_2(CO)_{11}$ ($d(PP) = 2.636$ Å) reversibly forms adducts with two-electron donor ligands.²⁸ The latter reactivity may be due to a $Fe-Fe$ double bond in this cluster.

With respect to intracluster $MG\cdots MG$ contacts, compounds **2**, $1 \cdot PPh_3$, and $Co_4Te_2(CO)_{11}$ constitute an intermediate class of

(32) Vahrenkamp, H.; Wucherer, E. J. *Angew. Chem., Int. Ed. Engl.* **1981**, *20*, 680.

(33) Khattab, S. A.; Markö, L.; Bor, G.; Markö, B. J. *Organomet. Chem.* **1964**, *1*, 373.

(34) Llabres, G.; Dideberg, O.; Dupont, L. *Acta Crystallogr., Sect. B* **1972**, *28B*, 2438.

(35) Cherin, P.; Unger, P. *Acta Crystallogr.* **1967**, *23*, 670.

(36) Burns, R. C.; Gillespie, R. J.; Luk, W. C.; Slim, D. R. *Inorg. Chem.* **1979**, *18*, 3086.

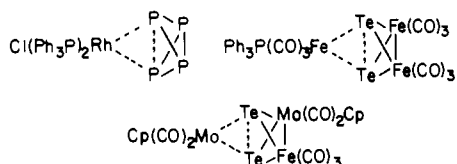
(37) Bottcher, P.; Kretschmann, V. Z. *Anorg. Allg. Chem.* **1982**, *491*, 39.

(38) Wei, C. H.; Dahl, L. F. *Cryst. Struct. Commun.* **1975**, *4*, 583.

(39) Pittman, C. U., Jr.; Wileman, G. M.; Wilson, W. D.; Ryan, R. C. *Angew. Chem., Int. Ed. Engl.* **1980**, *19*, 478.

(TM)_x(MG)₃ cluster compounds. At one extreme lie the "innocent" (MG)₂-containing clusters with no MG...MG interaction, exemplified by Cp₃Co₃S₂⁴⁰ and Cp₃Ni₃S₂.⁴¹ At the other extreme lie clusters with very short intracuster MG...MG contacts exemplified by E₂[W(CO)₅]₃ (E = As, Sb, and Bi). The compound Bi₂W₃(CO)₁₅ features a Bi...Bi distance of 2.818 Å, which indicates acetylene-like multiple Bi-Bi bonding.^{3c} The relationship of **2** to this latter group is further evidenced by its oxidation to form a derivative which has an even shorter Te-Te bond.¹⁷ Finally, we note that the increase in MG-MG bond order upon going from Cp₃Co₃S₂ to **2** and then to Bi₂W₃(CO)₁₅ is accompanied by a decrease in net M-M bond order.

An alternative view of the bonding in **2** and in related arachno clusters is suggested by a recent report on the structure of Rh-(P₄)(PPh₃)₂Cl.⁴² In this complex the 14e⁻ Rh(PPh₃)₂Cl fragment



binds in an η² fashion to the P₄ tetrahedron, elongating this edge by 0.25 Å. The coordinated P atoms remain mutually bonded, and the elongation of the P-P bond is analogous to that observed for olefin and acetylene coordination. The core of Fe₂(Te₂)(CO)₆ is similar structurally and electronically to P₄ as are the As_n(Co(CO)₃)_{4-n} clusters.⁴³ From this perspective it is clear that

(40) Frisch, P. D.; Dahl, L. F. *J. Am. Chem. Soc.* 1972, 94, 5082.

(41) Uchtman, V. A.; Vahrenkamp, H.; Dahl, L. F. *J. Am. Chem. Soc.* 1968, 90, 3272.

(42) Lindsell, W. E.; McCullough, K. J.; Welch, A. J. *J. Am. Chem. Soc.* 1983, 105, 4487.

(43) (a) Foust, A. S.; Foster, M. S.; Dahl, L. F. *J. Am. Chem. Soc.* 1969, 91, 5631. (b) Foust, A. S.; Foster, M. S.; Dahl, L. F. *J. Am. Chem. Soc.* 1969, 91, 5633. (c) Vizi-Orosz, A.; Galamb, V.; Pályi, G.; Markó, L.; Bor, G.; Natile, G. *J. Organomet. Chem.* 1976, 107, 235.

the "oxidative addition" of Fe₂(Te₂)(CO)₆ to Fe(CO)₃PPh₃ may be more appropriately described as coordination of largely intact Te-Te bond to the 16e⁻ Fe(CO)₃PPh₃ fragment. In the same way, **2** may be considered to be derived from the coordination of [CpMoFe(μ-η²-Te₂)(CO)₅]⁺¹⁷ to [CpMo(CO)₂]⁻.⁴⁴

Acknowledgment. This research was supported by the National Science Foundation (NSF CHE 81-06781). T.B.R. acknowledges fellowships from the A. P. Sloan and the Camille and Henry Dreyfus Foundations. L.E.B. is a UIF fellow. The National Science Foundation supported the purchase of the University of Delaware diffractometer. Field desorption and fast atom bombardment mass spectra were obtained in the Mass Spectrometry Laboratory of the School of Chemical Sciences at the University of Illinois, supported in part by a grant from the National Institute of General Medical Sciences (GM 27029). The ZAB-HF mass spectrometer was purchased in part with grants from the Division of Research Resources, National Institutes of Health (RR 01575), and the National Science Foundation (PCM-8121494).

Registry No. 1, 22587-70-8; 2, 94820-11-8; 2', 94820-12-9; 3, 94843-04-6; 3'', 94843-05-7; Cp₂Mo₂Fe₂Te₃(CO)₆, 94820-13-0; Cp₂Mo₂FeTe(CO)₇, 94820-14-1; Cp'₂Mo₂Fe₂Te₃(CO)₆, 94820-15-2; Cp'₂Mo₂FeTe(CO)₇, 94820-16-3; Cp₃Mo₂CoFeTe₂(CO)₅ (isomer I), 94820-18-5; Cp₃Mo₂CoFeTe₂(CO)₅ (isomer II), 94820-17-4; Fe₃S₂(C-O)₉, 22309-04-2; Co₂FeTe(CO)₉, 35163-37-2; CpMoCoFeTe(CO)₈, 94843-06-8; CpMo(CO)₃Br, 12079-79-7; Cp₂Mo₂(CO)₆, 12091-64-4; Cp'₂Mo₂(CO)₆, 33056-03-0; Fe(CO)₅, 13463-40-6; CpCo(CO)₂, 12078-25-0; Fe₂S₂(CO)₆, 14243-23-3; Co₂(CO)₈, 15226-74-1; Cp₂Mo₂(CO)₄, 56200-27-2.

Supplementary Material Available: Atomic coordinates, bond lengths, bond angles, anisotropic temperature factors, hydrogen atom coordinates, and structure factor tables (F_o vs. F_c) (89 pages). Ordering information is given on any current masthead page.

(44) Publication of this paper was delayed at the authors' request.

Mononuclear and Binuclear Cationic Complexes of Vanadium(II)

F. Albert Cotton,*[†] Stan A. Duraj,[†] Leo E. Manzer,[†] and Wieslaw J. Roth[†]

Contribution from the Department of Chemistry and Laboratory for Molecular Structure and Bonding, Texas A&M University, College Station, Texas 77843, and Central Research and Development Department, E. I. DuPont de Nemours & Company, Wilmington, Delaware 19898. Received December 11, 1984

Abstract: A method for the high-yield synthesis (up to 99%) of the new compounds [(THF)₃V(μ-Cl)₃V(THF)₃]AlCl₂R₂, where R = Et or Me, is described. Compound **1**, R = Et, reacts instantaneously with methanol to give a blue solution from which, depending upon the workup, [V(CH₃OH)₆]Cl₂ (**3**) or VCl₂(CH₃OH)₄ (**2**) can be obtained. With trimethylphosphine **1** readily affords [(PMe₃)₃V(μ-Cl)₃V(PMe₃)₃]AlCl₂Et₂ (**4**). Crystals of **1** diffracted poorly, and the structure could not be satisfactorily refined because of severe disorder in the tetrahydrofuran ligands as well as in the diethyldichloroaluminate anion. The structure was solved, however, and refined sufficiently to define the tri(μ-chloro)hexa(tetrahydrofuran)divanadium(II) cation and the diethyldichloroaluminate anion unambiguously but not accurately. Further characterization came from elemental analysis on all six elements of **1** and its UV spectrum. Compound **3** crystallizes in space group P2₁/n with the following unit cell dimensions: a = 6.993 (3) Å, b = 10.809 (4) Å, c = 10.298 (4) Å, β = 97.00 (3)°, V = 764.8 (9) Å³, Z = 2. [V(MeOH)₆]Cl₂ represents the first example of a homoleptic vanadium(II) alcoholate to be fully characterized by X-ray crystallography. For compound **4** the orthorhombic unit cell (space group Pnma) has the following dimensions: a = 12.705 (2) Å, b = 12.522 (4) Å, c = 28.554 (9) Å, V = 4543 (3) Å³, and Z = 4. The V-V distance in **4** is 3.103 (4) Å.

Our knowledge of the nonaqueous chemistry of vanadium in very low valence states (I, II), but not involving cyclopentadienyl

and/or carbonyl ligands, is still very inadequate. One important reason for this is the lack of suitable (easily prepared, soluble in common organic solvents, etc.) starting materials. For some time it was believed that "VCl₂(THF)₂" would be a good choice, but this compound proved, via X-ray crystallographic studies, to be

[†]Texas A&M University.

[†]E. I. DuPont de Nemours & Company.